Available online at www.sciencedirect.com
ScienceDirect
International Journal of Heat and Fluid Flow 28 (2007) 838–845
International Journal of HEAT AND FLUID FLOW
www.elsevier.com/locate/ijhff

# Flow of Giesekus viscoelastic fluid in a concentric annulus with inner cylinder rotation

Maryam Takht Ravanchi, Mahmoud Mirzazadeh, Fariborz Rashidi *

*Chemical Engineering Department, Amirkabir University of Technology, Hafez Ave., No. 424, Tehran, Iran*

Received 9 September 2005; received in revised form 25 April 2006; accepted 14 August 2006
Available online 13 November 2006

**Abstract**

An approximate analytical solution is derived for the steady state, purely tangential flow of a viscoelastic fluid obeying the Giesekus constitutive equation in a concentric annulus with inner cylinder rotation. An approximation is used for the estimation of radial normal stress. The effect of Weissenberg number (*We*), radius ratio ($\kappa$) and mobility factor ($\alpha$) on velocity distribution and *fRe* are investigated. The results show that the velocity gradient near the inner cylinder increases as the fluid elasticity increases. The results also show that *fRe* decreases with increasing fluid elasticity.
© 2006 Elsevier Inc. All rights reserved.

*Keywords:* Giesekus model; Tangential flow; Viscoelastic fluid

## 1. Introduction

Tangential flows of non-Newtonian fluids within annuli have wide range of engineering applications such as to journal bearings, commercial viscometers, swirl nozzles, chemical and mechanical mixing equipment and electrical motors (Maron and Cohen, 1991). An extensive bibliography of papers on the flow of non-Newtonian liquids through annular channels is given in a recent paper by Escudier et al. (2002). The tangential flow of Maxwell, White–Metzner and CEF fluids in concentric and eccentric annuli has been analyzed using perturbation theory (Beris et al., 1983). The flow of a Casson fluid between two rotating cylinders was studied by Batra and Das (1992) and a summary of laminar flow of non-Newtonian fluids in a rotating annulus was reported by Batra and Eissa (1994). Flow of a fluid obeying the Robertson–Stiff model was investigated by Eissa and Ahmad (1999), while Rao (1999) reported results for the flow of a Johnson–Segalman fluid between rotating co-axial cylinders. Khellaf and Lauriat (2000) analyzed the convective heat transfer characteristics for the flow of a Carreau fluid between rotating concentric vertical cylinders. Cruz and Pinho (2004) derived an analytical solution for helical flow within a concentric annulus of a fluid obeying the simplified form of the Phan–Thien–Tanner (SPTT) constitutive equation. An analytical solution is derived for the tangential flow of a viscoelastic fluid obeying the Phan–Thien–Tanner (PTT) constitutive equation in a concentric annulus with relative rotation of the inner and outer cylinders (Mirzazadeh et al., 2005).

Giesekus (1982) has developed a three-parameters model using molecular ideas that is nonlinear in the stresses. This model has gained prominence because it describes the power-law regions for viscosity and normal-stress coefficients; it also gives a reasonable description of the elongational viscosity and the complex viscosity. This model incorporates shear-thinning shear viscosity, non-vanishing normal-stress differences; extensional viscosity with finite asymptotic value and non-exponential stress relaxation and start-up curves. It reproduces thus many of the characteristics of the rheology of polymer solutions and other liquids.

* Corresponding author. Tel.: +98 21 6499066; fax: +98 21 6405847.
*E-mail address:* rashidi@aut.ac.ir (F. Rashidi).

0142-727X/$ - see front matter © 2006 Elsevier Inc. All rights reserved.
doi:10.1016/j.ijheatfluidflow.2006.08.003

**Nomenclature**

| | |
|---|---|
| $A$, $B$ | constants [see Eqs. (29) and (30)] |
| $C_2$ | constant of integration in velocity profile [Eq. (28)] |
| $f$ | rotational friction factor, $\tau_w/(\rho v_c^2/2)$ |
| $r$ | radial coordinate (m) |
| $R_i$ | radius of inner cylinder, $\kappa R$ |
| $R_o$ | radius of outer cylinder |
| $Re$ | rotational Reynolds number, $\rho v_c \delta/\eta$ |
| $Ta$ | Taylor number, $(\rho\Omega/\eta)^2 R_i \delta^3$ |
| $T$ | torque (N m) |
| $v_c$ | characteristic velocity, $\kappa R\Omega$ |
| $V_\theta$ | tangential velocity (m/s) |
| $We$ | Weissenberg number, $\lambda v_c/\delta$ |
| $z$ | axial coordinate (m) |
| $\alpha$ | mobility factor |
| $\lambda$ | relaxation time in Giesekus model (s) |
| $\rho$ | fluid density |
| $\kappa$ | radius ratio |
| $\delta$ | annular gap between annulus cylinders |
| $\Omega$ | angular velocity of inner cylinder ($s^{-1}$) |
| $\tau$ | stress tensor (Pa) |
| $\dot{\gamma}$ | shear rate tensor ($s^{-1}$) |
| $\eta$ | viscosity coefficient of the Giesekus model (Pa s) |
| $\theta$ | tangential coordinate |

*Superscripts*

| | |
|---|---|
| T | transpose of tensor |
| * | refers to dimensionless quantities |

*Subscripts*

| | |
|---|---|
| i | refers to inner cylinder |
| N | refers to Newtonian value |
| w | refers to wall value |

Performance of the Giesekus model in start-up flow in simple shear has also been studied to show its capability in predicting stress overshoots as observed in experiments (Giesekus, 1983).

The Giesekus model is being employed increasingly to predict the flow and heat transfer of viscoelastic fluids: recent papers include those of Yoo and Choi (1989); Schleiniger and Weinacht (1991) and Mostafaiyan et al. (2004).

The objective of the present paper is to report velocity profiles as well as the coefficient of friction using an analytical method to solve the Giesekus model in purely tangential flow between concentric rotating cylinders where the inner cylinder is rotating and outer cylinder is at rest, for a wide range of Weissenberg numbers and aspect ratios.

## 2. Governing equations

By assuming steady state, purely tangential laminar flow and neglecting body forces we have

$$v_\theta = v_\theta(r), \quad v_r = v_z = 0 \tag{1}$$

where $v_\theta$, $v_z$ and $v_r$ are the tangential, axial and radial components of velocity. Under these conditions the radial and tangential momentum equations are given as follows:

$$-\rho\frac{v_\theta^2}{r} = \frac{1}{r}\frac{\partial}{\partial r}(r\tau_{rr}) - \frac{\tau_{\theta\theta}}{r} - \frac{\partial p}{\partial r} + \frac{1}{r}\frac{\partial \tau_{r\theta}}{\partial \theta} \tag{2}$$

$$\frac{1}{r^2}\frac{\partial}{\partial r}(r^2\tau_{r\theta}) + \frac{1}{r}\frac{\partial p}{\partial \theta} + \frac{1}{r}\frac{\partial \tau_{\theta\theta}}{\partial \theta} = 0 \tag{3}$$

Since the considered geometry is the concentric rotating cylinder then it will be azimuthally symmetric, thus all of the differentials which are with respect to $\theta$ will be discarded from Eqs. (2) and (3). Then the above equations are reduced to

$$-\rho\frac{v_\theta^2}{r} = \frac{1}{r}\frac{\partial}{\partial r}(r\tau_{rr}) - \frac{\tau_{\theta\theta}}{r} - \frac{\partial P}{\partial r} \tag{2-a}$$

$$\frac{1}{r^2}\frac{\partial}{\partial r}(r^2\tau_{r\theta}) = 0 \tag{3-a}$$

where $\tau_{rr}$, $\tau_{\theta\theta}$ and $\tau_{r\theta}$ are the components of the stress tensor and $r$, $z$ and $\theta$ refer to the radial, axial and tangential directions, respectively.

The boundary conditions for this problem arise from no-slip at the walls and are given by

$$r = \kappa R, \quad v_\theta = \kappa R\Omega \tag{4}$$

$$r = R, \quad v_\theta = 0 \tag{5}$$

The Giesekus model which is used as the rheological model is as follows:

$$\tau + \frac{\alpha\lambda}{\eta}(\tau\cdot\tau) + \lambda\tau_{(1)} = \eta\dot{\gamma} \tag{6}$$

where

$$\dot{\gamma} = 2D = \left[\nabla v + (\nabla v)^{\mathrm{T}}\right] \tag{7}$$

$$\tau_{(1)} = \frac{D\tau}{Dt} - \left\{\tau\cdot\nabla v + (\nabla v)^{\mathrm{T}}\cdot\tau\right\} \tag{8}$$

$$\frac{D\tau}{Dt} = \frac{\partial\tau}{\partial t} + (v\cdot\nabla)\tau \tag{9}$$

$\eta$ and $\lambda$ are the model parameters and represent zero-shear viscosity and zero-shear relaxation time, respectively (Giesekus, 1983). The parameter $\alpha$ in Eq. (6) is a model parameter and the term containing $\alpha$ in the constitutive equation has been attributed to anisotropic Brownian motion and/or anisotropic hydrodynamic drag on the constituent polymer molecules (Bird et al., 1987) and it is required that $0 \leqslant \alpha \leqslant 1$ as discussed in (Giesekus, 1982). Setting $\alpha = 0$ reduces the model to the upper convected Maxwell.

## 3. Approximate solution

By introducing the following dimensionless quantities:

$$\tau^* = \frac{\tau}{\eta v_c/\delta}, \quad \dot{\gamma}^* = \frac{\dot{\gamma}}{v_c/\delta} \tag{10}$$

$$v_\theta^* = \frac{v_\theta}{v_c} \tag{11}$$

$$We = \frac{\lambda v_c}{\delta} \tag{12}$$

$$r^* = \frac{r}{R} \tag{13}$$

where $v_c$ is the characteristic velocity and defined as $\kappa R\Omega$, $\delta$ is the annular gap and is equal to $R(1-\kappa)$ and $R$ is the radius of outer cylinder while $\kappa$ is the radius ratio.

Integration of Eq. (3-a) after non-dimensionalisation leads to

$$\tau_{r\theta}^* = \frac{\kappa^2 \tau_{wi}^*}{r^{*2}} \tag{14}$$

where $\tau_{wi}^*$ is the dimensionless wall shear stress on the inner cylinder.

By expanding the Giesekus constitutive equation (Eq. (6)) for steady tangential annular flow where $\dot{\gamma} = r\mathrm{d}(v_\theta/r)/\mathrm{d}r$, we arrive at

$$\tau_{rr}^* + \alpha We(\tau_{rr}^{*2} + \tau_{r\theta}^{*2}) = 0 \tag{15}$$

$$\tau_{r\theta}^* - We\dot{\gamma}^*\tau_{rr}^* + \alpha We\tau_{r\theta}^*(\tau_{\theta\theta}^* + \tau_{rr}^*) = \dot{\gamma}^* \tag{16}$$

$$\tau_{\theta\theta}^* - 2We\dot{\gamma}^*\tau_{r\theta}^* + \alpha We(\tau_{\theta\theta}^{*2} + \tau_{r\theta}^{*2}) = 0 \tag{17}$$

Eq. (15) is second order with respect to $\tau_{rr}^*$, hence:

$$\tau_{rr}^* = \frac{-1 \pm \sqrt{1 - 4\alpha^2 We^2 \tau_{r\theta}^{*2}}}{2\alpha We} \tag{18}$$

The classical positive and negative solutions of Eq. (18) have been discussed by Schleiniger and Weinacht (1991) using linear stability analysis and the requirements arising from configuration tensor. They concluded that for the case of no-solvent viscosity there is only one stable physically relevant solution and that is the positive solution with the following restrictions:

$$|\tau_{r\theta}^*| < \frac{1}{We}\sqrt{\frac{1}{\alpha} - 1}, \quad 0 < \alpha \leqslant \frac{1}{2} \tag{19}$$

$$|\tau_{r\theta}^*| \leqslant \frac{1}{2\alpha We}, \quad \frac{1}{2} < \alpha \leqslant 1 \tag{20}$$

Yoo and Choi (1989) used a different approach for stability analysis. They concluded for the case of no-solvent solution and in order to obtain a real solution for the normal stress (Eq. (18)) it is necessary to apply the following condition:

$$1 - 4\alpha^2 We^2 \tau_{r\theta}^{*2} \geqslant 0 \tag{21}$$

In addition to this, the first normal stress difference ($\tau_{\theta\theta} - \tau_{rr}$) must be positive from thermodynamic considerations. Applying of these conditions arrived at the same conclusion as Eqs. (19) and (20).

For the present study and by substitution of $\tau_{r\theta}^*$ from Eq. (14) into Eqs. (19) and (20) we then have

$$|\tau_{wi}^*| < \frac{r^{*2}}{\kappa^2 We}\sqrt{\frac{1}{\alpha} - 1}, \quad 0 < \alpha \leqslant \frac{1}{2} \tag{22}$$

$$|\tau_{wi}^*| < \frac{r^{*2}}{2\kappa^2 \alpha We}, \quad \frac{1}{2} < \alpha \leqslant 1 \tag{22-a}$$

Since $\kappa \leqslant r^* \leqslant 1$ then Eqs. (22) and (22-a) leads to

$$|\tau_{wi}^*| < \frac{1}{We}\sqrt{\frac{1}{\alpha} - 1} \tag{23}$$

$$|\tau_{wi}^*| < \frac{1}{2\alpha We}, \quad \frac{1}{2} < \alpha \leqslant 1 \tag{23-a}$$

These inequalities implicitly indicate the conditions beyond which there are real solutions for tangential flow of a fluid obeying the Giesekus constitutive equation.

From Eq. (16), $\tau_{\theta\theta}^*$ is

$$\tau_{\theta\theta}^* = \frac{1 + We\tau_{rr}^*}{\alpha We\tau_{r\theta}^*}\dot{\gamma} - \frac{1 + \alpha We\tau_{rr}^*}{\alpha We} \tag{24}$$

Combining Eqs. (15), (17) and (24) leads to

$$\dot{\gamma}^* = \frac{1 + (2\alpha - 1)We\tau_{rr}^*}{(1 + We\tau_{rr}^*)^2}\tau_{r\theta}^* \tag{25}$$

where the $\dot{\gamma}^*$ is equal to $(1-\kappa)r^*\frac{\mathrm{d}}{\mathrm{d}r^*}\left(\frac{v_\theta^*}{r^*}\right)$.

In the approximate solution approach, the term $\sqrt{1 - 4\alpha^2 We^2 \tau_{r\theta}^{*2}}$ in Eq. (18) can be expressed in a power series, using the binominal expansion:

$$\sqrt{1 - 4\alpha^2 We^2 \tau_{r\theta}^{*2}} \cong 1 - 2\alpha^2 We^2 \tau_{r\theta}^{*2} \tag{26}$$

where all terms of higher order have been neglected compared to the leading term, in the approximation, which is valid approximation for the small value of $4\alpha^2 We^2 \tau_{r\theta}^{*2}$. The truncation error is less than 6% when $4\alpha^2 We^2 \tau_{r\theta}^{*2}$ is less than $\frac{1}{2}$ (6% relative to the exact value of, $\sqrt{1 - 4\alpha^2 We^2 \tau_{r\theta}^{*2}}$). Therefore when $4\alpha^2 We^2 \tau_{r\theta}^{*2} < \frac{1}{2}$ (or $|\tau_{wi}^*| < \frac{1}{2\sqrt{2}\alpha We}$) the accuracy of approximation is more than 94%. Whereas in this inequality $\tau_{wi}^*$ is a function of $We$ and $\alpha$ (which will be shown in Eqs. (29)–(31)), therefore this inequality implicitly indicates the conditions beyond which there are acceptable approximation errors. So in any case both of the constitutive stability condition (Eqs. (23) and (23-a)) and the approximation validity condition (i.e. $|\tau_{wi}^*| < \frac{1}{2\sqrt{2}\alpha We}$) should be satisfied simultaneously. Comparison of these conditions for a given value of $We$ and $\alpha$ indicates that when $\alpha$ is less than 0.14645 the estimated value of $|\tau_{wi}^*|$ from the stability condition (Eq. (23)) is smaller than the estimated value of $|\tau_{wi}^*|$ from the approximation validity condition and when $\alpha$ is greater than 0.14645 the trend is opposite. In other word for lower value of mobility factor ($\alpha < 0.14645$) satisfying the stability condition is enough and for higher value of $\alpha$ we just need to check the approximation validity condition.

The dimensionless radial normal stress $\tau^*_{rr}$ can be obtained by substitution of Eq. (26) into Eq. (18):

$$\tau^*_{rr} = -\alpha We \tau^{*2}_{r\theta} \tag{27}$$

Substitution of Eqs. (14) and (27) into Eq. (25) followed by integration leads to the dimensionless form of the velocity profile:

$$\frac{v^*_\theta}{r^*} = \frac{1}{4}\left(\frac{A}{B}-1\right)\frac{\kappa^2\tau^*_{wi}}{1-\kappa}\frac{r^{*2}}{r^{*4}-B\tau^{*2}_{wi}} - \frac{1}{4}\frac{\kappa^2}{\sqrt{B}(1-\kappa)}\left(1+\frac{A}{B}\right)\arctan h\left(\frac{r^{*2}}{\tau^*_{wi}\sqrt{B}}\right)+C_2 \tag{28}$$

where

$$A = \alpha(2\alpha-1)We^2\kappa^4 \tag{29}$$

$$B = \alpha We^2\kappa^4 \tag{30}$$

By introducing boundary conditions from Eqs. (4) and (5) into Eq. (28), the following relation can be derived:

$$\frac{1}{\kappa} = \frac{\kappa^2\tau^*_{wi}}{4(1-\kappa)}\left(\frac{A}{B}-1\right)\left[\frac{\kappa^2}{\kappa^4-B\tau^{*2}_{wi}}-\frac{1}{1-B\tau^{*2}_{wi}}\right] - \frac{\kappa^2}{4\sqrt{B}}\left(\frac{A}{B}+1\right)\left[\arctan h\left(\frac{\kappa^2}{\tau^*_{wi}\sqrt{B}}\right)-\arctan h\left(\frac{1}{\tau^*_{wi}\sqrt{B}}\right)\right] \tag{31}$$

Eq. (31) is strongly nonlinear but can be solved numerically for the dimensionless wall shear stress $\tau^*_{wi}$ on the inner cylinder. The Newton–Raphson method is used for the solution of Eq. (31) where the Newtonian value of $\tau^*_{wi}$ (which is obtained in the next paragraph, Eq. (33)) is used as an initial guess. Once $\tau^*_{wi}$ is known, determination of constant $C_2$ in Eq. (28) is straightforward: $C_2$ is obtained from Eq. (28) and by applying one of the boundary conditions (Eq. (4) or Eq. (5)).

For the limiting case of Newtonian fluid ($We \to 0$ and $\alpha \to 0$), A and B in Eqs. (29) and (30) approach to zero and the ratio of $A/B$ goes to $(-1)$, then the second term on the right hand side of Eqs. (28) and (31) will be zero. Therefore these equations reduce to

$$\frac{v^*_\theta}{r^*} = -\frac{1}{2}\frac{\kappa^2\tau^*_{wi}}{(1-\kappa)}\frac{1}{r^{*2}}+C_2 \tag{32}$$

$$\frac{1}{\kappa} = \frac{\kappa^2\tau^*_{wi}}{4(1-\kappa)}(-2)\left[\frac{1}{\kappa^2}-1\right] \quad \text{or} \quad \tau^*_{wi} = -\frac{2}{\kappa(1+\kappa)} \tag{33}$$

And $C_2$ for this case can be obtained from Eq. (32) and by applying one of the boundary conditions (Eq. (4) or (5)).

$$C_2 = -\frac{\kappa}{1-\kappa^2} \tag{34}$$

Substitution of Eqs. (33) and (34) into Eq. (32) results in the following equation for the velocity profile of Newtonian fluid which is in total agreement with the previous work (see e.g. Bird et al., 1987)

$$\frac{v^*_\theta}{r^*} = \frac{\kappa}{1-\kappa^2}\left(\frac{1}{r^{*2}}-1\right) \tag{35}$$

An important parameter in engineering calculations is the torque friction factor $f$ defined as $f = \tau_{wi}/(\rho v_c^2/2)$. As is usual, we evaluate the product of $f$ and the rotational Reynolds number $Re$ which is defined as $Re = \rho v_c \delta/\eta$ (Vohr, 1968). Using these definitions we can derive the following equations for the product of the torque friction factor and the rotational Reynolds number:

$$fRe = -2\tau^*_{wi} \tag{36}$$

The Taylor number, $Ta$, is an alternative to the rotational Reynolds number and for the case of inner cylinder rotation, it is defined as follows (Escudier et al., 2002):

$$Ta = \left(\frac{\rho\Omega}{\eta}\right)^2 R_i\delta^3 \tag{37}$$

Using the torque friction factor and the Taylor number, the following correlation will be gained:

$$f\sqrt{Ta} = -2\tau^*_{wi}\sqrt{\frac{1-\kappa}{\kappa}} \tag{38}$$

## 4. Results and discussion

Figs. 1 and 2 show the effect of the Weissenberg number and mobility factor ($\alpha$) on the velocity profile. As can be seen, the velocity gradient near the inner cylinder increases as the two parameters increase, i.e. as the shear-thinning behavior of the fluid increases.

The effect of fluid elasticity on dimensionless shear stress is shown in Fig. 3, which again indicates the shear-thinning behavior of Giesekus model. But Fig. 4 shows that the normal stress ($\tau_{rr}$) does not behave monotonically, in other

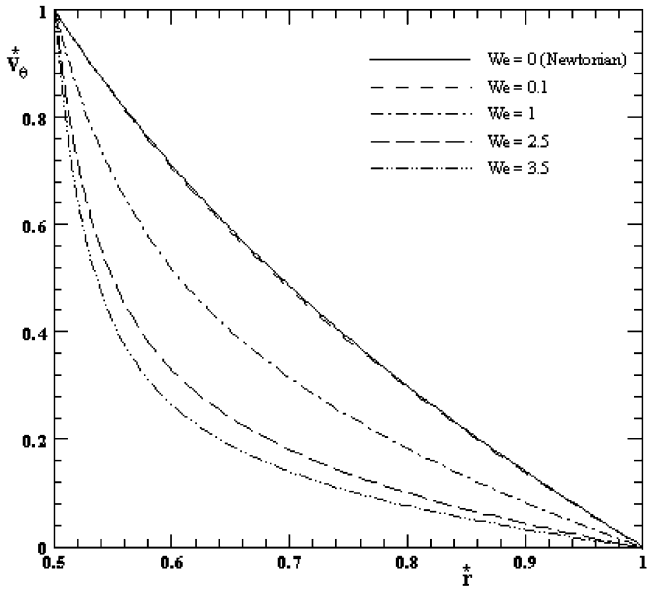


Fig. 1. Velocity profiles for constant values of $\alpha = 0.2$, $\kappa = 0.5$ and different values of $We$.

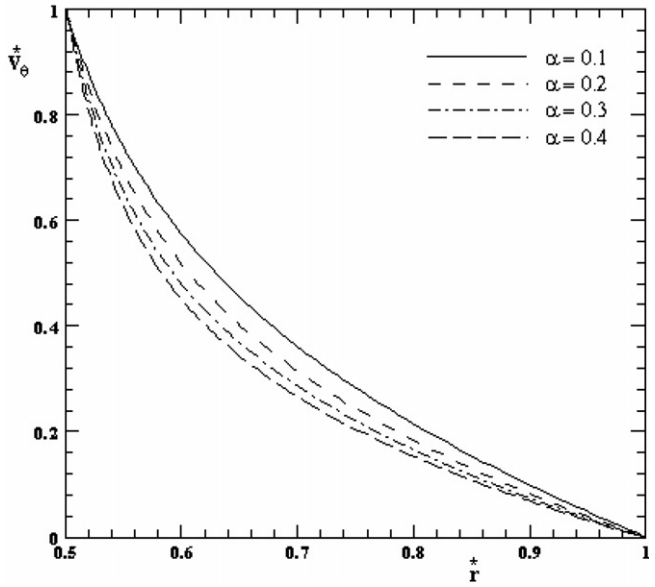


Fig. 2. Velocity profiles for constant values of $We = 1$, $\kappa = 0.5$ and different values of $\alpha$.

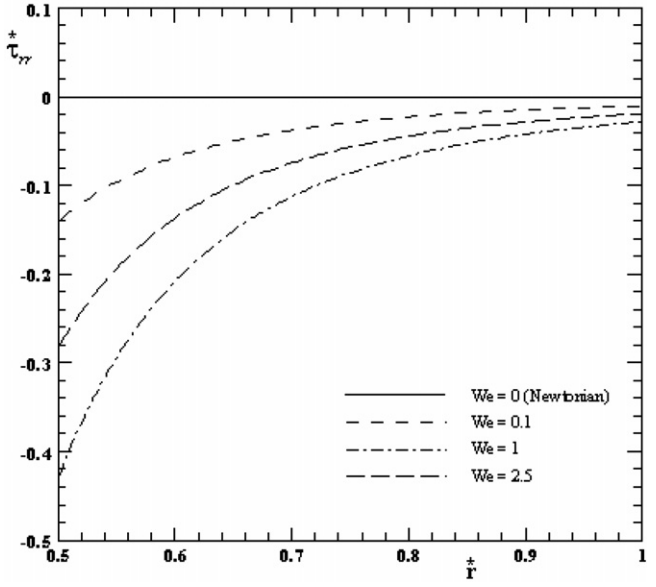


Fig. 4. The effect of $We$ on radial profile of dimensionless normal stress ($\tau^*_{rr}$) for constant values of $\alpha = 0.2$, $\kappa = 0.5$.

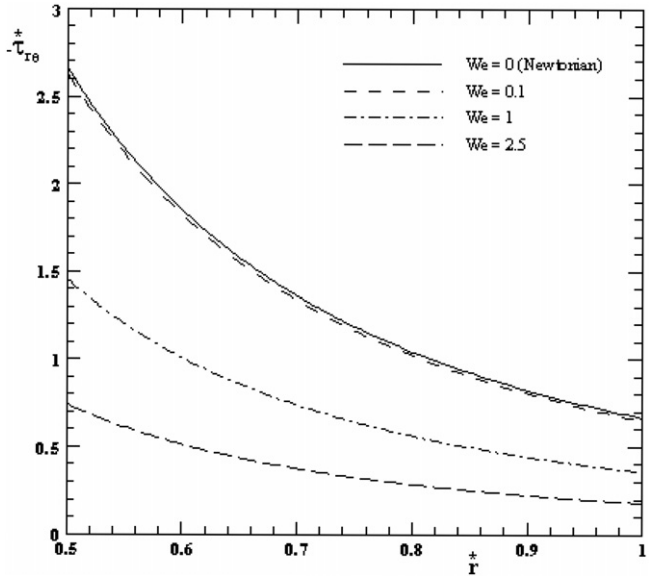


Fig. 3. The effect of fluid elasticity on shear stress for constant values of $\alpha = 0.2$, $\kappa = 0.5$ and different values of $We$.

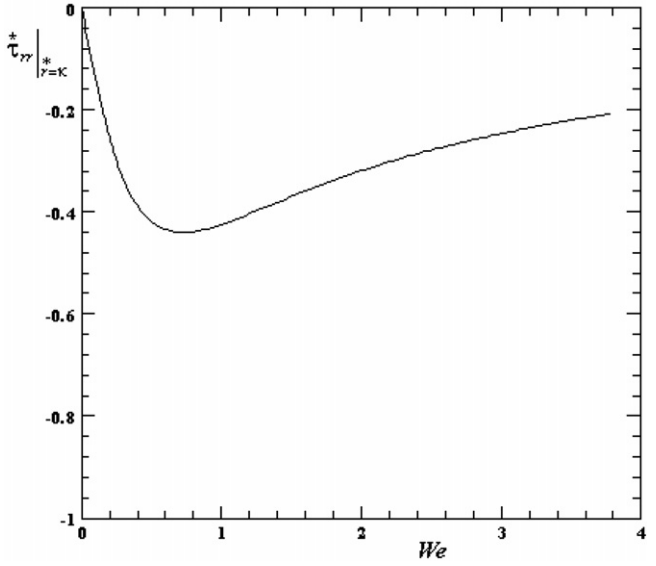


Fig. 5. $\tau^*_{rr}|_{r^*=\kappa}$ vs. $We$ for constant values of $\alpha = 0.2$, $\kappa = 0.5$.

word the absolute value of $\tau^*_{rr}$ first increases by increasing Weissenberg number but when Weissenberg number goes to higher values it shows the opposite trend (as it shown in Fig. 5, where the value of $\tau^*_{rr}$ on the inner cylinder is shown against Weissenberg number). This is because $\tau^*_{rr}$ is affected by both of fluid elasticity (directly proportional to $We$, as can be seen from Eq. (27)) and by shear-thinning behavior of fluid (as it shown in Fig. 3, where $\tau^*_{r\theta}$ decreases by increasing fluid elasticity). For this reason it would be better to plot the normal stress scaled with wall shear stress as it shown in Fig. 6, as can be seen from this figure the shear-thinning effect is removed from the normal-stress profile. A similar result has been obtained previously by Oliveira (2002) for pipe and slit flow of FENE-P fluid (Fig. 4a in his work), Mostafaiyan et al. (2004) for annular flow of Giesekus fluid (Fig. 2a in their work) and also by Oliveira and Pinho (1999) for channel and pipe flow of PTT fluid (Fig. 4b in their work).

Fig. 7 shows the effect of fluid elasticity on the azimuthally component of normal stress ($\tau^*_{\theta\theta}$), A similar conclusion to that for $\tau^*_{rr}$ can be reached for this case. In this figure the relation between $\tau^*_{\theta\theta}$ and fluid parameters (e.g. fluid elasticity and mobility factor) can be obtained from the below equation and after some mathematical simplification:

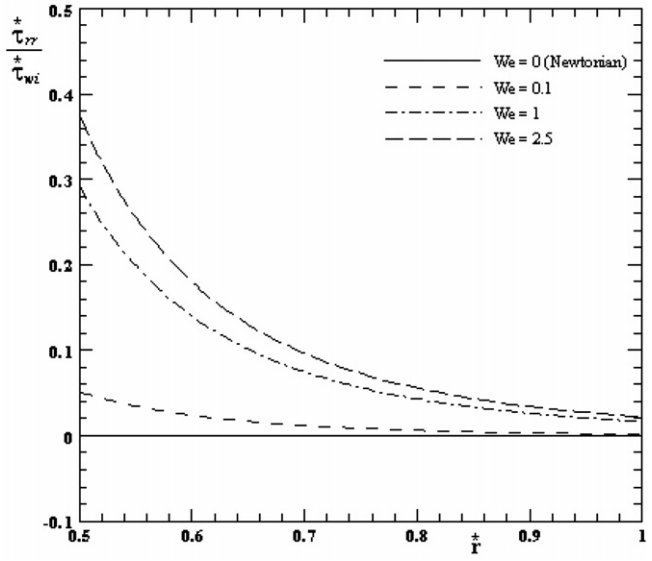


Fig. 6. Dimensionless normal-stress profiles for varying Weissenberg number normalized with dimensionless wall shear stress ($\tau^*_{wi}$) for constant values of $\alpha = 0.2$, $\kappa = 0.5$.

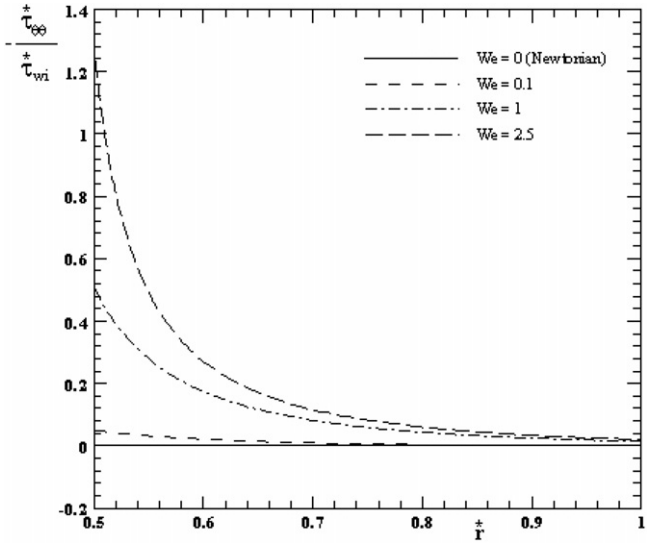


Fig. 7. Dimensionless normal-stress profiles for varying Weissenberg number normalized with dimensionless wall shear stress ($\tau^*_{wi}$) for constant values of $\alpha = 0.2$, $\kappa = 0.5$.

$$\tau^*_{\theta\theta} = \frac{(1-\alpha)\left(-1 \pm \sqrt{1 - 4\alpha^2 We^2 \tau^{*2}_{r\theta}}\right) + 2\alpha^2 We^2 \tau^{*2}_{r\theta}}{\alpha We\left[2\alpha - 1 \pm \sqrt{1 - 4\alpha^2 We^2 \tau^{*2}_{r\theta}}\right]} \tag{39}$$

Using the similar approximation approach for $\sqrt{1 - 4\alpha^2 We^2 \tau^{*2}_{r\theta}}$, and by substitution of $\sqrt{1 - 4\alpha^2 We^2 \tau^{*2}_{r\theta}}$ from Eq. (26) into Eq. (39) we arrive at the following equation for $\tau^*_{\theta\theta}$:

$$\tau^*_{\theta\theta} = \frac{\alpha We \tau^{*2}_{r\theta}}{1 - \alpha We^2 \tau^{*2}_{r\theta}} \tag{40}$$

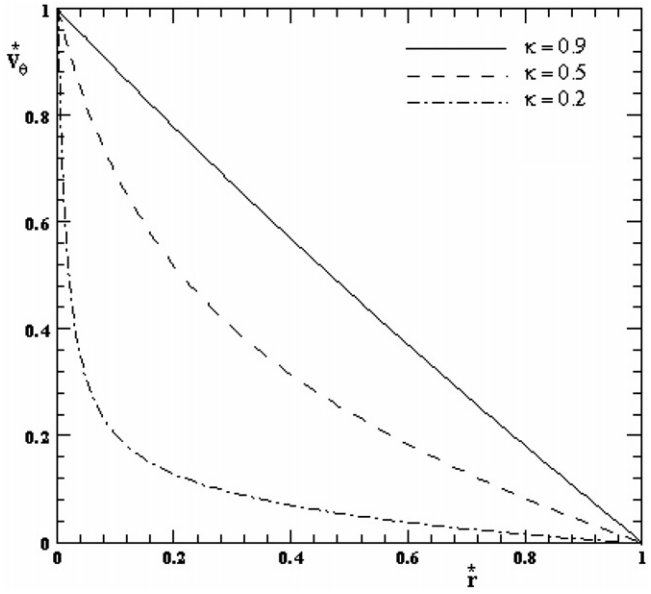


Fig. 8. The effect of radius ratio on the velocity profile for constant values of $\alpha = 0.2$, $We = 1$ and different values of $\kappa$.

The influence of the radius ratio on the velocity profile is shown in Fig. 8. These results show that the profiles become increasingly linear with increasing $\kappa$.

Figs. 9 and 10 show the effect the Weissenberg number and mobility factor ($\alpha$) on $fRe$ which is normalized with the corresponding Newtonian value ($fRe_N = 4/\kappa(1+\kappa)$). The decrease in $fRe$ with increasing elasticity is again attributable to the shear-thinning behavior of the Giesekus fluid. Also it can be seen from Fig. 9, as Weissenberg number approaches zero the $fRe$ values are in agreement with those for a Newtonian fluid (Khellaf and Lauriat, 2000; Vohr, 1968; Gazley and Monica, 1956).

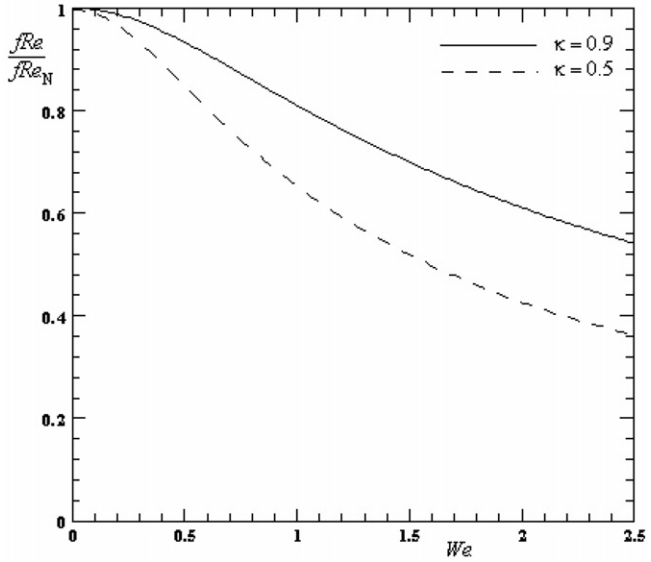


Fig. 9. The effect of $We$ on the ratio of viscoelastic to Newtonian friction factor ($fRe/fRe_N$) for $\alpha = 0.2$ and different values of $\kappa$.

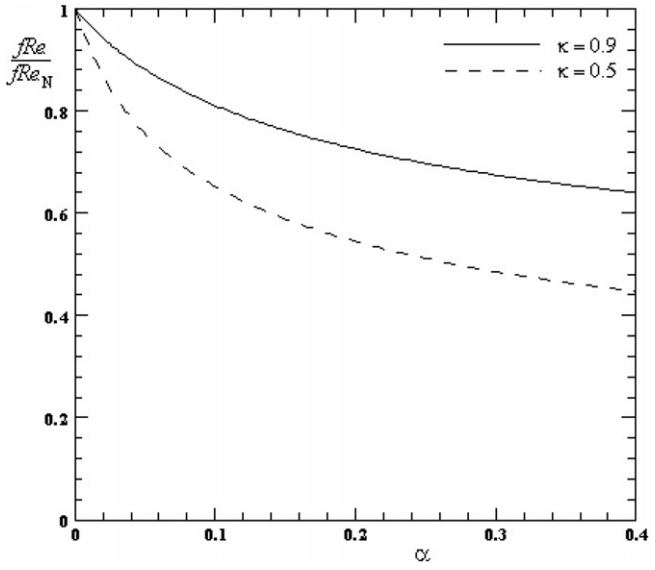


Fig. 10. The effect of $\alpha$ on ratio of viscoelastic to Newtonian friction factor ($fRe/fRe_N$) for $We = 1$ and different values of $\kappa$.

From an engineering perspective, a useful piece of information is the development of torque versus angular velocity (or Weissenberg number). The torque $T$ is given by

$$T = -\tau_{r\theta}|_{r=R_i}(2\pi R_i L)R_i \tag{41}$$

If the value of $T$ for the Giesekus fluid is normalized with the corresponding Newtonian value, $T_N$ then

$$\frac{T}{T_N} = \frac{\tau^*_{wi}}{\tau^*_{wi,N}} = \frac{fRe}{(fRe)_N} \tag{42}$$

which indicates that the effects of $We$, $\kappa$ and $\alpha$ on torque are identical to the effects of these parameters on $fRe$. As a consequence, increasing fluid elasticity decreases the required torque for rotation of the cylinders.

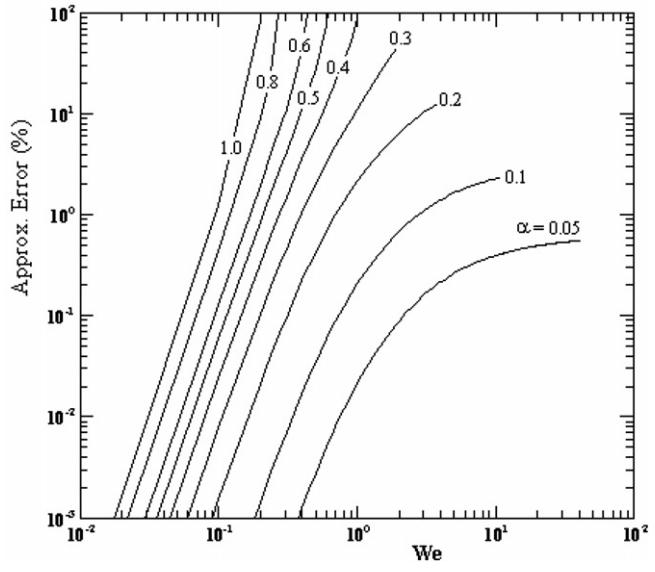


Fig. 11. The map of approximation validity for different value of $We$ and $\alpha$ and for $\kappa = 0.5$.

Fig. 11 presents the percentage of truncation error as function of Weissenberg number and mobility factor. As can be seen from this figure by increasing the value of $\alpha$ the range of acceptable Weissenberg number becomes narrower. Whereas the approximate solution is valid for the small value of $(4\alpha^2 We^2 \tau^{*2}_{r\theta})$, therefore any increase in the value of $\alpha$ and $We$ results in increase in the percentage of truncation error. Also as it shown in this figure for each $\alpha$, and regardless of the percentage of truncation error, there is an upper limit for Weissenberg number based on the stability criterion (see Eqs. (23) and (23-a)). For example for $\alpha < 0.2$, even though the percentage of truncation error is very small but we can't go to very high Weissenberg number because of stability limitation. A similar conclusion was achieved by Yoo and Choi (1989) (see Figs. 4 and 6 in their work).

## 5. Conclusion

An approximate analytical solution has been derived for the steady state, purely tangential flow in a concentric annulus of a viscoelastic fluid obeying the Giesekus constitutive equation. The results show that increasing the Weissenberg number and mobility factor increases the velocity gradient near the inner cylinder and so decreases the viscometric viscosity of the fluid (i.e. the fluid behavior is increasingly shear thinning). The competing effect of fluid elasticity and shear-thinning behavior of fluid results in the non-monotonically trend of the normal stresses. The results also show that $fRe$ and the required torque for rotation of inner cylinder decreases with increasing fluid elasticity. With increasing radius ratio the velocity profile tends to take a linear form.

## References

Batra, R.L., Das, B., 1992. Flow of Casson fluid between two rotating cylinder. Fluid Dynamics Research 9, 133–141.

Batra, R.L., Eissa, M., 1994. Helical flow of a Sutterby model fluid. Polymer – Plastics Technology and Engineering 33, 489–501.

Beris, A.N., Armstrong, R.C., Brown, R.A., 1983. Perturbation theory for viscoelastic fluids between eccentric rotating cylinders. Journal of Non-Newtonian Fluid Mechanics 13, 109–143.

Bird, R.B., Armstorng, R.C., Hassager, O., 1987. Dynamics of polymeric liquids, second ed.Fluid Dynamics, vol. 1 Wiley, New York.

Cruz, D.O.A., Pinho, F.T., 2004. Skewed Poiseuille–Couette low of SPTT fluids in concentric annuli and channels. Journal of Non-Newtonian Fluid Mechanics 121, 1–14.

Eissa, M., Ahmad, S., 1999. Forced convection heat transfer of Robertson–Stiff fluid between two coaxial rotating cylinders. International Communication in Heat and Mass Transfer 26, 695–704.

Escudier, M.P., Oliveira, P.J., Pinho, F.T., 2002. Fully developed laminar flow of purely viscous non-Newtonian liquids through annuli including the effects of eccentricity and inner cylinder rotation. International Journal of Heat and Fluid Flow 23 (1), 52–73.

Gazley Jr., C., Monica, C.S., 1956. Heat transfer characteristics of the rotational and axial flow between concentric cylinders. Transactions of The ASME, paper number 56-A-128, November 25, pp. 79–90.

Giesekus, H., 1982. A simple constitutive equation for polymer fluids based on the concept of deformation-dependent tonsorial mobility. Journal of Non-Newtonian Fluid Mechanics 11, 69–109.

Giesekus, H., 1983. Stressing behavior in simple shear flow as predicted by a new consecutive model for polymer fluids. Journal of Non-Newtonian Fluid Mechanics 12, 367–374.

Khellaf, K., Lauriat, G., 2000. Numerical study of heat transfer in a non-Newtonian Carreau-fluid between rotating concentric vertical cylinders. Journal of Non-Newtonian Fluid Mechanics 89, 45–61.

Maron, D.M., Cohen, S., 1991. Hydrodynamics and heat/mass transfer near rotating surfaces. Advances in Heat Transfer 21, 141–183.

Mirzazadeh, M., Rashidi, F., Hashemabadi, S.H., 2005. Purely tangential flow of a PTT-viscoelastic fluid within a concentric annulus. Journal of Non-Newtonian Fluid Mechanics 129, 88–97.

Mostafaiyan, M., Khodabandehlou, Kh., Sharif, F., 2004. Analysis of a viscoelastic fluid in an annulus using Giesekus model. Journal of Non-Newtonian Fluid Mechanics 118, 49–55.

Oliveira, P.J., 2002. An exact solution for tube and slit flow of a FENE-P fluid. Acta Mechanica 158, 1–11.

Oliveira, P.J., Pinho, F.T., 1999. Analytical solution for fully developed channel and pipe flow of Phan–Thien–Tanner fluids. Journal of Fluid Mechanics 387, 271–280.

Rao, I.J., 1999. Flow of a Johnson–Segalman fluid between rotating coaxial cylinders with and without suction. International Journal of Non-Linear Mechanics 34, 63–70.

Schleiniger, G., Weinacht, R., 1991. Steady Poiseuille flows for a Giesekus fluid. Journal of Non-Newtonian Fluid Mechanics 40, 79–102.

Vohr, J.H., 1968. An experimental study of the Taylor vortices and turbulence in flow between eccentric rotating cylinders. Journal of Lubrication Technology 90, 285–296.

Yoo, J.Y., Choi, H.Ch., 1989. On the steady simple shear flows of the one-mode Giesekus fluid. Rheologica Acta 28, 13–24.